Semiclassical treatment of matter-enhanced neutrino oscillations for an arbitrary density profile

A. B. Balantekin* and J. F. Beacom†
Department of Physics, University of Wisconsin, Madison, Wisconsin 53706
(Received 17 June 1996)

The matter-enhanced oscillations of two neutrino flavors are studied using a uniform semiclassical approximation. Unlike some analytic studies which have focused on certain exactly solvable densities, this method can be used for an arbitrary monotonic density profile. The method is applicable to a wider range of mixing parameters than previous approximate methods for arbitrary densities. The approximation is excellent in the adiabatic regime and up to the extreme nonadiabatic limit. In particular, the range of validity for this approximation extends farther into the nonadiabatic regime than for the linear Landau-Zener result. This method also allows calculation of the source- and detector-dependent terms in the unaveraged survival probability, and analytic results for these terms are given. These interference terms may be important in studying neutrino mixing in the Sun or in supernovas. [S0556-2821(96)01722-5]

PACS number(s): 14.60.Pq, 03.65.Sq, 26.65.+t, 96.60.Jw

I. INTRODUCTION

Matter-enhanced oscillations of neutrino flavors via the Mikheyev-Smirnov-Wolfenstein (MSW) mechanism [1] have been studied for neutrinos in various environments, but most extensively for the Sun, in connection with the solar neutrino problem [2]. For a recent review of the solar neutrino problem and the ongoing neutrino detection experiments, see Ref. [3]. Recently, interest has also been developing for the study of neutrino oscillations in supernovas [4].

The approximate results derived in this paper are applicable to matter-enhanced, two-flavor neutrino oscillations in general physical situations. Analytic results are important for several reasons. While numerical integration of the MSW equations is straightforward, it becomes extremely tedious when it must be done for a large range of the mixing parameters. Analytic results also allow a greater understanding of the effects of changes in the parameters, and may be useful for extracting information about the solar density from the measured neutrino fluxes.

Analytic studies of matter-enhanced neutrino oscillations proceed along two lines. The first approach is the study of certain densities for which an exact solution for the oscillation probability can be obtained. The mixing parameters are allowed to be arbitrary. The exponential density has attracted particular interest, since it approximates the solar density. A catalog of all of the exactly solvable densities has been presented in Ref. [5]. The second approach allows for a general density, but restricts the parameters so that an approximation can be made to the equations of motion, which are then solved exactly. The approximations are chosen so that the exact results are recovered in either the extreme nonadiabatic or extreme adiabatic limit. In this paper, we consider a uniform semiclassical approximation to derive the neutrino conversion probability for an arbitrary density. The solution is exact in the adiabatic limit, such as the linear Landau-Zener result. However, the new result has a larger range of validity in the nonadiabatic regime. In the body of the paper, we will discuss how some of the different approximations are related.

II. MATTER-ENHANCED NEUTRINO OSCILLATIONS

A. Coupled equations in the flavor basis

For two neutrino flavors (taken here to be electron and muon) in matter, the equations of motion for the ν_e and ν_μ probability amplitudes in the relativistic limit are

$$i\hbar\frac{\partial}{\partial t}\begin{bmatrix}\Psi_e(t)\\ \Psi_\mu(t)\end{bmatrix}=\frac{1}{4E}\begin{bmatrix}A-\delta m^2\cos 2\theta_v & \delta m^2\sin 2\theta_v\\ \delta m^2\sin 2\theta_v & -A+\delta m^2\cos 2\theta_v\end{bmatrix}\times\begin{bmatrix}\Psi_e(t)\\ \Psi_\mu(t)\end{bmatrix}, \tag{2.1}$$

where all terms in the Hamiltonian proportional to the identity have been dropped since they do not contribute to the relative phase between the ν_e and ν_μ components. The vacuum-mixing parameters are specified by the vacuum-mixing angle θ_v, taken to be $0<\theta_v<\pi/4$, and the vacuum mass-squared splitting $\delta m^2\equiv m_2^2-m_1^2$, where we take $m_2>m_1$. Electron neutrinos experience charged-current scattering with the electrons in the medium, whereas muon neutrinos do not. This difference yields the effective mass correction

$$A=2\sqrt{2}G_F N_e(t)E, \tag{2.2}$$

where G_F is the Fermi constant and $N_e(t)$ is the number density of electrons in the medium.

Before proceeding further, we switch to working with dimensionless quantities. We define a length scale

$$L=\frac{\hbar\lambda}{\delta m^2/4E}, \tag{2.3}$$

and use this to define $x=t/L$. Since we will be making a semiclassical expansion, we need to be able to keep track of

*Electronic address: baha@nucth.physics.wisc.edu
†Electronic address: beacom@nucth.physics.wisc.edu

formal powers of $\hbar$. For each $\hbar$ in the problem, we write λ and consider λ to be formally small; this is equivalent to saying that the length L is small. We will make expansions in powers of λ, truncating the higher orders. At the end of the calculation, we will set $\lambda=1$. For notational convenience, we write

$$i\lambda\frac{\partial}{\partial x}\begin{bmatrix}\Psi_e(x)\\ \Psi_\mu(x)\end{bmatrix}=H_{e\mu}(x)\begin{bmatrix}\Psi_e(x)\\ \Psi_\mu(x)\end{bmatrix}=\begin{bmatrix}\eta\varphi(x) & \sqrt{\Lambda}\\ \sqrt{\Lambda} & -\eta\varphi(x)\end{bmatrix}\times\begin{bmatrix}\Psi_e(x)\\ \Psi_\mu(x)\end{bmatrix}. \tag{2.4}$$

We have defined

$$\eta\varphi(x)=\zeta(x)-\cos 2\theta_v \tag{2.5}$$

and

$$\Lambda=\sin 2\theta_v\,. \tag{2.6}$$

The scaled electron density is

$$\zeta(x)=\zeta(x_i)N_e(x)/N_e(x_i), \tag{2.7}$$

normalized at the initial point x_i as

$$\zeta(x_i)=\frac{2\sqrt{2}G_F E N_e(x_i)}{\delta m^2}. \tag{2.8}$$

Note that there are notation changes from Refs. [6–8]; here, we have made Λ and φ dimensionless. The factor η (taken to be ±1), is introduced above to control the analytic behavior of the function $\varphi(x)$ in the complex plane, as explained in Appendix. In the expressions with φ^2 below, we drop $\eta^2=1$.

B. Coupled equations in the adiabatic basis

The flavor-basis Hamiltonian of Eq. (2.4) can be instantaneously diagonalized. We make a change of basis

$$\begin{bmatrix}\Psi_1(x)\\ \Psi_2(x)\end{bmatrix}=R(-\theta(x))\begin{bmatrix}\Psi_e(x)\\ \Psi_\mu(x)\end{bmatrix}=\begin{bmatrix}\cos\theta(x) & -\sin\theta(x)\\ \sin\theta(x) & \cos\theta(x)\end{bmatrix}\times\begin{bmatrix}\Psi_e(x)\\ \Psi_\mu(x)\end{bmatrix}. \tag{2.9}$$

$\Psi_1(x)$ is the probability amplitude to be in the ''light'' (primarily electron-type) eigenstate in the mass basis, and $\Psi_2(x)$ is the probability amplitude to be in the ''heavy'' (primarily muon-type) eigenstate in the mass basis. The requirement that this transformation instantaneously diagonalize $H_{e\mu}(x)$ defines the matter-mixing angle via

$$\sin 2\theta(x)=\frac{\sqrt{\Lambda}}{\sqrt{\Lambda+\varphi^2(x)}} \tag{2.10}$$

and

$$\cos 2\theta(x)=\frac{-\eta\varphi(x)}{\sqrt{\Lambda+\varphi^2(x)}}. \tag{2.11}$$

The matter angle thus ranges from $\pi/2$ at infinite density to θ_v in vacuum. At the resonance, $\theta=\pi/4$. The instantaneous eigenvalues of $H_{e\mu}(x)$ are

$$\mp\sqrt{\Lambda+\varphi^2(x)}, \tag{2.12}$$

corresponding to Ψ_1 (the ''light'' eigenstate) and Ψ_2 (the ''heavy'' eigenstate), respectively. The splitting between the instantaneous mass eigenstates has a minimum as a function of x when $\varphi(x)=0$, or $\zeta(x)=\cos2\theta_v$; this is the MSW resonance point, which will be denoted by x_c. The trajectories of these eigenvalues represent an avoided level crossing. The adiabatic limit is the case where the neutrino stays in one of the instantaneous eigenstates during its entire propagation. In the nonadiabatic limit, the neutrino may ''hop'' from one eigenstate to the other near the resonance.

In the mass basis, the equations of motion are

$$i\lambda\frac{\partial}{\partial x}\begin{bmatrix}\Psi_1(x)\\ \Psi_2(x)\end{bmatrix}=H_{12}(x)\begin{bmatrix}\Psi_1(x)\\ \Psi_2(x)\end{bmatrix}=\begin{bmatrix}-\sqrt{\Lambda+\varphi^2(x)} & -i\lambda\theta'(x)\\ i\lambda\theta'(x) & \sqrt{\Lambda+\varphi^2(x)}\end{bmatrix}\begin{bmatrix}\Psi_1(x)\\ \Psi_2(x)\end{bmatrix}. \tag{2.13}$$

Throughout the paper, prime denotes derivative with respect to x. When the density is changing slowly, then so is the matter angle $\theta(x)$, and the off-diagonal terms can be neglected; for that reason, this is also known as the ''adiabatic'' basis. The adiabaticity parameter is defined as

$$\gamma(x)=\left|\frac{\sqrt{\Lambda+\varphi^2(x)}}{i\lambda\theta'(x)}\right|, \tag{2.14}$$

where $\theta'(x)$ can be derived from Eqs. (2.10) and (2.11). When this parameter $\gamma(x)$ is large, we can neglect the off-diagonal terms. All nonadiabatic behavior, i.e., hopping from one mass eigenstate to the other, takes place in a neighborhood of the resonance. It is there that $\gamma(x)$ is minimized, so the requirement of $\gamma(x)\gg1$ for adiabatic propagation is the most exacting:

$$\gamma_c=\gamma(x_c)=\frac{2}{\lambda}\frac{\sin^2 2\theta_v}{\cos 2\theta_v}\frac{1}{|\zeta'/\zeta|_{x_c}}\gg1\,. \tag{2.15}$$

In this limit, the equations of motion can be integrated immediately, yielding pure phases for $\Psi_1(x)$ and $\Psi_2(x)$. At the initial point x_i, we take the neutrino to be a pure ν_e, so

$$\Psi_e(x_i)=1 \tag{2.16}$$

and

$$\Psi_e'(x_i)=\left.\frac{\partial\Psi_e(x)}{\partial x}\right|_{x_i}=-\frac{i}{\lambda}\eta\varphi(x_i). \tag{2.17}$$

The latter follows from $\Psi_e(x_i)=1$, $\Psi_\mu(x_i)=0$. We denote the initial matter angle by θ_i and reference the phases from the initial point x_i. The phase integral will be denoted by

$$I_p(x,x_i)\equiv\int_{x_i}^{x}dx\sqrt{\Lambda+\varphi^2(x)}. \tag{2.18}$$

Taking into account the basis changes at the initial and final points, the adiabatic solutions, valid in the limit $\gamma(x_c)\gg 1$, are

$$\Psi_e(x)=\cos\theta(x)\cos\theta_i\exp\left(+\frac{i}{\lambda}I_p(x,x_i)\right)+\sin\theta(x)\sin\theta_i\exp\left(-\frac{i}{\lambda}I_p(x,x_i)\right) \tag{2.19}$$

and

$$\Psi_\mu(x)=-\sin\theta(x)\cos\theta_i\exp\left(+\frac{i}{\lambda}I_p(x,x_i)\right)+\cos\theta(x)\sin\theta_i\exp\left(-\frac{i}{\lambda}I_p(x,x_i)\right). \tag{2.20}$$

These forms hold both before and after the resonance in the adiabatic limit. If nonadiabatic corrections are taken into account, then the wave functions will have these forms before the resonance but will be more complicated after the resonance. In the adiabatic limit [9], the electron neutrino survival probability at a general point x is

$$P(\nu_e\to\nu_e)(x,x_i)=|\Psi_e(x)|^2=\frac{1}{2}[1+\cos 2\theta_i\cos 2\theta(x)]+\frac{1}{2}\sin 2\theta_i\sin 2\theta(x)\cos\left(\frac{2}{\lambda}I_p(x,x_i)\right). \tag{2.21}$$

Note that the second term depends upon the source and detector positions, and will disappear under averaging of either. The probability of conversion to muon-type is given by $P(\nu_e\to\nu_\mu)=1-P(\nu_e\to\nu_e)$. If the final point is chosen in vacuum, then $\theta(x)\to\theta_v$.

With the adiabatic limit in hand, the obvious thing to do is to seek the corrections that take into account $P_{\rm hop}$, the probability of hopping from one mass eigenstate to the other. Above, the adiabatic approximation was controlled by the ratio of diagonal to off-diagonal elements. That ratio is, in turn, controlled by λ, which keeps track of powers of $\hbar$. In the semiclassical limit of $\hbar\to 0$, one has $\lambda\to 0$ and $\gamma_c\to\infty$. Note that λ appears above in the adiabatic survival probability only in the phase; the fully averaged expression is independent of λ. The way to treat $P_{\rm hop}$ systematically is to expand in powers of λ and to keep only the lowest-order terms.

C. Uncoupled equations in the flavor basis

The coupled first-order equations for the flavor-basis wave functions can be decoupled to yield

$$-\lambda^2\frac{\partial^2\Psi_e(x)}{\partial x^2}-[\Lambda+\varphi^2(x)+i\lambda\,\eta\varphi'(x)]\Psi_e(x)=0 \tag{2.22}$$

and

$$-\lambda^2\frac{\partial^2\Psi_\mu(x)}{\partial x^2}-[\Lambda+\varphi^2(x)-i\lambda\,\eta\varphi'(x)]\Psi_\mu(x)=0, \tag{2.23}$$

where $\varphi(x)$ and Λ are defined in Eqs. (2.5) and (2.6), respectively. Such a simple decoupling is not possible in the matter basis.

These Schrödinger-like equations are similar to those for nonrelativistic particles in the presence of a complex barrier, and for convenience we use the language of wave mechanics to describe them. In particular, to the extent that we can ignore the imaginary terms in the potential, these correspond to particles above a barrier (since $\Lambda>0$). There are two caveats regarding discussing this as a barrier penetration problem. First, that our boundary conditions do not correspond to the usual picture of incident, reflected, and transmitted waves; in general, there are waves moving in each direction on each side of the barrier. Second, the pure imaginary terms in the potentials play an extremely important role here, even in the asymptotic regions. These terms are needed not only to represent nonadiabatic transitions, but also to keep up with the local matter angle.

In this problem, then, the quantity of interest is not a reflection or transmission coefficient, but rather $P(\nu_e\to\nu_e)=|\Psi_e(x\to\infty)|^2$, the probability of the neutrino being of the electron-type far from the source. In general, this is a function of both source and detector positions, though typically, only the fully averaged result is presented. However, those interference terms could be important, and we present approximate expressions for them in the next section.

Two well-known semiclassical treatments of this problem are via the Wentzel-Kramers-Brillouin (WKB) [7] and linear Landau-Zener [10–12] methods. The WKB technique *globally* maps the ''potential'' discussed above onto the free-particle potential (i.e., a constant density). By ''global mapping,'' we mean a variable stretching of the axis that deforms the shape of one potential into another. In fact, the WKB treatment turns out to be identical to the adiabatic approximation [7]. The linear Landau-Zener technique *locally* maps onto a linear density (i.e., extends a linear profile from a single MSW resonance point with the right density and derivative), and hence a ''potential'' with a parabolic real part and constant imaginary part. While the linear Landau-Zener result is easy to derive and apply, there are two problems. First, it is notoriously difficult to get the boundary conditions right (for a complete explanation of how to handle this, see Ref. [13]). Second, since Landau-Zener is a point mapping, the expression for $P_{\rm hop}$ is not very accurate. In the case of neutrino oscillations in the Sun, the exponential Landau-Zener approximation circumvents these problems [13].

The aim of this paper is to calculate the nonadiabatic corrections semiclassically, but with a *global* mapping of the ''potential,'' where, as in the Landau-Zener calculation we choose as a model the case of a linear density. By using a global mapping, the correct boundary conditions are auto-

matic. Further, the expression for $P_{\rm hop}$ is more accurate. The approximate wave function is uniformly valid in x (though the approximation is not uniform in the mixing parameters).

III. UNIFORM SEMICLASSICAL SOLUTION OF THE MSW EQUATIONS

A. Semiclassical background

In the adiabatic limit, only the lowest order is kept in the limit $\lambda \to 0$ in Eq. (2.13), so the Hamiltonian is taken as diagonal (no hopping from one mass eigenstate to the other) and the integration is trivial. The treatment at that order suggests that in order to take into account the probability of hopping, we will need to consider further orders in λ. In this section, we will show that it is possible to obtain a rather accurate expression for the electron neutrino survival probability by making a semiclassical expansion, i.e., by considering only the two lowest orders in λ when solving the MSW equations.

The expressions derived below will hold for values of the mixing parameters from the extreme adiabatic limit up until the extreme nonadiabatic limit. In order to obtain solutions that hold in the extreme nonadiabatic limit, one would formally have to consider all orders in λ. Since semiclassical expansions are asymptotic (i.e., nonconvergent) in general, it is not clear that this would work in practice. A much better approach for the extreme nonadiabatic limit is to consider expansions in $1/\lambda$ [14].

Semiclassical methods (for reviews, see Ref. [15]) are used in quantum mechanics to provide approximate solutions to the Schrödinger equation in the limit that λ is small. As noted, in the WKB method, one bases the approximate solutions on free-particle solutions. A procedure was developed by Miller and Good [16] that, instead, bases the approximate solutions on the known solutions of a Schrödinger equation with a similar potential. In this method, the turning-point singularities of the primitive WKB method are regulated, and the solutions are uniformly valid: they hold over the whole range in x and are well-behaved at the turning-points. A further advantage of the Miller-Good method is that different potentials are treated with the same formalism, i.e., the method of connection is the same for all potentials with the same number and type of turning points.

The MSW equations (2.22) and (2.23) are Schrödinger-type equations for particles in the presence of complex potentials of the form $V(x) = -[\varphi^2(x) \pm i\lambda\,\eta\varphi'(x)]$, with $\varphi(x)$ independent of λ. In Appendix, we summarize the extension of the uniform semiclassical approximation to treat potentials with this specific dependence on λ, originally introduced in Refs. [6–8]. This special form of the potential arises in supersymmetric quantum mechanics; see Ref. [8] for discussion.

B. Application to the MSW problem

The method presented in Appendix allows a uniform semiclassical solution for $\Psi_e(x)$. By ''uniform,'' we mean that the local error incurred by using the approximate solution developed there in the exact differential equation is bounded as a function of x. This is to be distinguished from a semiclassical solution via the primitive WKB method. Such a solution has an unbounded error near a turning point. For MSW propagation, the turning points are complex (they are near the resonance point). In the nonadiabatic limit, the turning points approach the real axis, which means that the WKB solutions are unable to represent any of the nonadiabatic behavior. In contrast, the uniform semiclassical approximation used here is excellent for all but the extreme nonadiabatic limit. Since we will make a semiclassical expansion, we explicitly show all factors of $\hbar$ (via λ). Either an increasing or a decreasing density can be considered, by proper choice of η.

From the derivation in Appendix, the general solution to Eq. (2.22) is

$$\Psi_e(x) = K(x)[AD_\nu(z(x)) + BD_\nu(-z(x))], \tag{3.1}$$

where

$$\nu = \frac{\eta - 1 - i\Omega/\lambda}{2}, \tag{3.2}$$

with

$$\Omega = \frac{2i}{\pi}\int_{x_0}^{x_0^*} dx\,\sqrt{\Lambda + \varphi^2(x)}. \tag{3.3}$$

The limits of integration above are the zeros of the integrand, chosen as described in the Appendix. The argument of the parabolic cylinder functions is given by

$$z(x) = \frac{1+i}{\sqrt{\lambda}}S(x) \approx \frac{1+i}{\sqrt{\lambda}}[S_0(x) + \lambda S_1(x)], \tag{3.4}$$

where $S_0(x)$ and $S_1(x)$ are described in the Appendix.

Given appropriate initial conditions, one can solve for A and B. In some situations, it may be useful to evaluate $\Psi_e(x)$ for all x. This requires evaluating the Γ function for a complex argument and the parabolic cylinder functions for a general complex order and argument. For general comments on routines available for the numerical evaluation of special functions, see Ref. [17]. The Γ function for a complex argument can be evaluated with CERNLIB [18]. General properties of the parabolic cylinder functions may be found in Refs. [19–22]. While library routines do exist for various special cases of the parabolic cylinder functions, to our knowledge there is nothing available that is general enough [23]. The technique[1] used here is to use the power series [22] for small $|z|$, the asymptotic series [20] for large $|z|$, and direct numerical integration of the defining differential equation with ODEPACK [24] for moderate $|z|$. Fortunately, one does not generally have to perform any integrations for the parabolic cylinder functions, as only the asymptotic forms are needed.

We will use the asymptotic forms at both the production and detection points. As shown below, this means that we assume adiabatic propagation at those two points. This matching is justified to the extent that the production and detection points are sufficiently far from the resonance point. In practice, these requirements do not present any difficul-

[1]The code is available, upon request, from the authors.

ties. Consider the Sun as an example, with neutrinos produced at the solar center. If the resonance is near the production point, or there is no resonance, then this implies that δm^2 is large and the entire propagation is adiabatic, except for extremely small mixing angles. If the resonance is at a very low density, i.e., approaching vacuum, then δm^2 is very small and our approximation breaks down for other reasons described below. Note that in the linear Landau-Zener treatment, one has to handle the final x point carefully since the density runs negative at large x, and $\theta(x)\to 0$, not θ_v. No such difficulties with the boundary value of the matter angle arise in the treatment given here.

The asymptotic forms developed below represent $\Psi_e(x)$ well for large but finite x. All of the expansions below are just to get outside of the resonance region; we do not take x so large that the matter angle is either $\pi/2$ or θ_v. More precisely (see the discussion in the Appendix), the approximate solutions are characterized by two scales, one set by $S_0(x)$ and the other by $\varphi(x)$. The function $S_0(x)$ is asymptotic outside the resonance region, whereas $\varphi(x)$ is not asymptotic until the density is zero or infinite. In this formulation, $S_0(x)$, but not $\varphi(x)$, will be taken to be asymptotic. This means that we have the control to connect opposite sides of the resonance region without having to take $x\to\pm\infty$, i.e., we do not have to extend the density profile indefinitely.

C. Asymptotic solutions and connection formulas

Using the definition of the matter angle given in Eqs. (2.10) and (2.11), we can rewrite the pre-exponential factors in the asymptotic solution of $\Psi_e(x)$, Eq. (A37). There are two cases, depending on how φ and η are chosen. The first case has $\varphi(x)=\cos 2\theta_v-\zeta(x), \eta=-1$, so

$$\left[\frac{\Lambda}{4[\Lambda+\varphi^2(x)]}\right]^{1/4}\left(\frac{\varphi+\sqrt{\Lambda+\varphi^2}}{\sqrt{\Lambda}}\right)^{+1/2}=\cos\theta(x), \tag{3.5}$$

and

$$\left[\frac{\Lambda}{4[\Lambda+\varphi^2(x)]}\right]^{1/4}\left(\frac{\varphi+\sqrt{\Lambda+\varphi^2}}{\sqrt{\Lambda}}\right)^{-1/2}=\sin\theta(x). \tag{3.6}$$

In the other case of $\varphi(x)=-2\cos\theta_v+\zeta(x), \eta=+1$, these are reversed. In either case, the prefactors associated with the various terms are

$$C_-:\cos\theta(x),\quad D_-:\sin\theta(x),$$
$$C_+:\sin\theta(x),\quad D_+:\cos\theta(x). \tag{3.7}$$

It is important to note that these will be evaluated at general values of x outside the resonance region; $|x|$ will not be so large that $\theta(x)\to\pi/2$ or $\theta(x)\to\theta_v$. The asymptotic wave functions are

$$\Psi_e(x\to-\infty)=C_-\cos\theta(x)\exp\left(+\frac{i}{\lambda}I_p(x,x_i)\right)+D_-\sin\theta(x)\exp\left(-\frac{i}{\lambda}I_p(x,x_i)\right), \tag{3.8}$$

and

$$\Psi_e(x\to+\infty)=C_+\sin\theta(x)\exp\left(-\frac{i}{\lambda}I_p(x,x_i)\right)+D_+\cos\theta(x)\exp\left(+\frac{i}{\lambda}I_p(x,x_i)\right). \tag{3.9}$$

From their form, we see immediately that the asymptotic wave functions represent adiabatic propagation. The coefficients $C_\pm, D_\pm$ still depend on η, which will allow us to consider increasing or decreasing densities. The phase integral function I_p is defined in Eq. (A12).

With the asymptotic wave function in this form, it is rather easy to apply the initial conditions. As before, we take the neutrino at the initial point x_i to be a pure ν_e, so

$$\Psi_e(x_i)=1 \tag{3.10}$$

and

$$\Psi_e'(x_i)=\left.\frac{\partial\Psi_e(x)}{\partial x}\right|_{x_i}=-\frac{i}{\lambda}\eta\varphi(x_i). \tag{3.11}$$

In either case regarding the signs of φ and η, one immediately obtains $C_-=\cos\theta_i$ and $D_-=\sin\theta_i$, so

$$\Psi_e(x\to-\infty)=\cos\theta(x)\cos\theta_i\exp\left(+\frac{i}{\lambda}I_p(x,x_i)\right)+\sin\theta(x)\sin\theta_i\exp\left(-\frac{i}{\lambda}I_p(x,x_i)\right), \tag{3.12}$$

which is, of course, the adiabatic solution given in Sec. II B.

We now turn to the evaluation of the coefficients C_+ and D_+ that are needed after the resonance. From the above and Eqs. (A39) and (A41),

$$C_-=\cos\theta_i=C\exp\left(+\frac{i}{\lambda}\mathrm{Re}I_p(x_i,x_0)\right)(Ae^{-i\nu\pi}+B), \tag{3.13}$$

$$D_-=\sin\theta_i=C\exp\left(-\frac{i}{\lambda}\mathrm{Re}I_p(x_i,x_0)\right)(Ae^{-i\nu\pi}). \tag{3.14}$$

These determine the coefficients A and B of the general solution:

$$A=D^{-1}\exp\left(+\frac{i}{\lambda}\mathrm{Re}I_p(x_i,x_0)\right)e^{i\nu\pi}\sin\theta_i, \tag{3.15}$$

$$B=C^{-1}\exp\left(-\frac{i}{\lambda}\mathrm{Re}I_p(x_i,x_0)\right)\cos\theta_i-D^{-1}\exp\left(+\frac{i}{\lambda}\mathrm{Re}I_p(x_i,x_0)\right)\sin\theta_i. \tag{3.16}$$

Then,

$$C_+ = 2iCD^{-1}e^{i\nu\pi}\sin\theta_i + \exp\left(-\frac{2i}{\lambda}\mathrm{Re}I_p(x_i,x_0)\right) \times e^{-i\nu\pi}\cos\theta_i, \tag{3.17}$$

$$D_+ = C^{-1}De^{-i\nu\pi}\cos\theta_i - \exp\left(+\frac{2i}{\lambda}\mathrm{Re}I_p(x_i,x_0)\right) \times e^{-i\nu\pi}\sin\theta_i, \tag{3.18}$$

where C and D are given in Eqs. (A42) and (A43).

The asymptotic forms of $\Psi_e(x)$ shown above are perfectly general, and depend only on the assumption of adiabatic propagation outside the resonance region. The heart of this problem is the connection of the asymptotic coefficients C_- and D_- to C_+ and D_+. That connection represents the integration of the solutions through the resonance region. In our case, that information is carried by the coefficients A and B of the general (but approximate, due to the mapping) solution in terms of parabolic cylinder functions.

D. Resonance transition coefficients

Above, the asymptotic wave functions were written in terms of the adiabatic solutions, which is convenient for applying initial conditions and deducing the connection formulas. Before squaring the asymptotic wave function to obtain the neutrino survival probability, it is convenient to rewrite the wave function in a slightly different form:

$$\begin{aligned}\Psi_e(x\to+\infty) &= C_+\sin\theta(x)\exp\left(-\frac{i}{\lambda}I_p(x,x_i)\right) \\ &\quad + D_+\cos\theta(x)\exp\left(+\frac{i}{\lambda}I_p(x,x_i)\right) \\ &= \left[c_1\sin\theta_i\exp\left(+\frac{i}{\lambda}\mathrm{Re}I_p(x_i,x_0)\right)\right. \\ &\quad \left. + c_2\cos\theta_i\exp\left(-\frac{i}{\lambda}\mathrm{Re}I_p(x_i,x_0)\right)\right] \\ &\quad \times\sin\theta(x)\exp\left(-\frac{i}{\lambda}\mathrm{Re}I_p(x,x_0)\right) \\ &\quad + \left[d_1\cos\theta_i\exp\left(-\frac{i}{\lambda}\mathrm{Re}I_p(x_i,x_0)\right)\right. \\ &\quad \left. + d_2\sin\theta_i\exp\left(+\frac{i}{\lambda}\mathrm{Re}I_p(x_i,x_0)\right)\right] \\ &\quad \times\cos\theta(x)\exp\left(+\frac{i}{\lambda}\mathrm{Re}I_p(x,x_0)\right).\end{aligned} \tag{3.19}$$

The terms inside the square brackets depend only on the source position x_i, whereas the terms outside depend only on the final position x. Since all of the adiabatic phases and matter angles for the asymptotic solutions are written explicitly, the matrix of coefficients given by c_1, c_2, d_1, d_2 represents only the nonadiabatic transitions in the resonance region. These coefficients change in the resonance region, but tend asymptotically to constants outside of it. Since the 2×2 Hamiltonian is Hermitian and traceless, the time-evolution operator must be a member of the SU(2) group. Thus, this matrix must assume the form

$$\begin{bmatrix} c_1 & c_2 \\ -c_2^* & c_1^* \end{bmatrix}, \tag{3.20}$$

where $|c_1|^2+|c_2|^2=1$.

By comparison to the forms of C_+ and D_+ in Eqs. (A38) and (A40), the new coefficients are easily found to be

$$c_1 = -\frac{\Gamma(-\nu)}{\sqrt{2\pi}}\left(\frac{\Omega}{\lambda}\right)^{-i\Omega/2\lambda+\eta/2}\left(\frac{e^{-i\pi/2}}{2}\right)^{\nu}\frac{e^{-3i\pi/4}}{\sqrt{2}} \times\exp\left(+\frac{i\Omega}{2\lambda}\right)2i\sin(\nu\pi), \tag{3.21}$$

$$c_2 = e^{-i\nu\pi}, \tag{3.22}$$

$$d_1 = -\frac{\sqrt{2\pi}}{\Gamma(-\nu)}\left(\frac{\Omega}{\lambda}\right)^{+i\Omega/2\lambda-\eta/2}\left(\frac{e^{-i\pi/2}}{2}\right)^{-\nu}e^{+3i\pi/4}\sqrt{2} \times\exp\left(-\frac{i\Omega}{2\lambda}\right)e^{-i\nu\pi}, \tag{3.23}$$

$$d_2 = -e^{-i\nu\pi}. \tag{3.24}$$

By analysis of two cases of $\eta=\pm1$ separately, one can show [19]

$$|\Gamma(-\nu)|^2\left(\frac{\Omega}{2\lambda}\right)^{\eta} = \frac{\pi}{\sinh(\Omega\pi/2\lambda)}, \tag{3.25}$$

$$\frac{2}{\pi}|\Gamma(-\nu)|^2\left(\frac{\Omega}{2\lambda}\right)^{\eta}|\sin(\nu\pi)|^2e^{-\Omega\pi/2\lambda} = 1-e^{-\Omega\pi/2\lambda}, \tag{3.26}$$

where ν is given by Eq. (A22). Using these relations, it may easily be verified explicitly that $d_1^*=c_1$ and $d_2^*=-c_2$, and that

$$|c_1|^2 = 1-e^{-\Omega\pi/\lambda}, \tag{3.27}$$

$$|c_2|^2 = e^{-\Omega\pi/\lambda}, \tag{3.28}$$

so $|c_1|^2+|c_2|^2=1$.

Starting with Eq. (2.13), one can determine how c_1 and c_2 depend on η, i.e., on whether the density is increasing or decreasing. One can show that c_1 must be independent of η, and that c_2 must change sign if η does. With the present form of c_1, this is not obvious. Define the phase of c_1 as

$$c_1 = |c_1|e^{i\alpha}. \tag{3.29}$$

An asymptotic series can be developed for this phase α. Using the special form of the Stirling expansion of the Γ function for purely imaginary argument given in Eqs. (6.1.43) and (6.1.44) of Ref. [19], one can show that the phase of c_1, in the limit Ω/λ is large, is

$$\alpha=-\sum_{n=1}^{\infty}\frac{(-1)^{n-1}B_{2n}}{2n(2n-1)}\left(\frac{2\lambda}{\Omega}\right)^{2n-1}, \tag{3.30}$$

where B_{2n} are Bernoulli numbers [19]. When a linear density is considered, this expression for the phase is equal to that given in Ref. [25]. We do not use this limit for the phase in general, since it requires that $\Omega/\lambda\gtrsim 1$, which is unnecessarily restrictive on the range of validity of our main approximation. Since this is independent of η, so is c_1. Note from the definition of ν in Eq. (A22) that $c_2=e^{-i\nu\pi}$ is, in fact, a real number, though it may be positive or negative, and changes sign if η does.

E. Calculation of $P(\nu_e\rightarrow\nu_e)$

The electron neutrino survival probability at a general point x after the resonance for a neutrino produced at x_i is given by the modulus squared of the amplitude $\Psi_e(x\rightarrow+\infty)$ for the neutrino to be of the electron type. First write

$$\begin{aligned}\Psi_e(x\rightarrow+\infty)=&\left[c_1\sin\theta_i\exp\left(+\frac{i}{\lambda}\mathrm{Re}I_p(x_i,x_0)\right)\right.\\&\left.+c_2\cos\theta_i\exp\left(-\frac{i}{\lambda}\mathrm{Re}I_p(x_i,x_0)\right)\right]\\&\times\sin\theta(x)\exp\left(-\frac{i}{\lambda}\mathrm{Re}I_p(x,x_0)\right)\\&+\left[c_1^*\cos\theta_i\exp\left(-\frac{i}{\lambda}\mathrm{Re}I_p(x_i,x_0)\right)\right.\\&\left.-c_2^*\sin\theta_i\exp\left(+\frac{i}{\lambda}\mathrm{Re}I_p(x_i,x_0)\right)\right]\\&\times\cos\theta(x)\exp\left(+\frac{i}{\lambda}\mathrm{Re}I_p(x,x_0)\right).\end{aligned} \tag{3.31}$$

After taking the squared modulus of this expression for $\Psi_e(x)$, and then reducing it, the survival probability takes the form

$$\begin{aligned}P(\nu_e\rightarrow\nu_e)(x,x_i)=&\frac{1}{2}[1+(1-2|c_2|^2)\cos 2\theta_i\cos 2\theta(x)]-\frac{1}{2}|c_1|c_2\sin 2\theta_i\cos 2\theta(x)\cos\left(\frac{2}{\lambda}\mathrm{Re}I_p(x_i,x_0)+\alpha\right)\\&+\frac{1}{2}\sin 2\theta_i\sin 2\theta(x)\cos\left(\frac{2}{\lambda}\mathrm{Re}I_p(x,x_i)-2\alpha\right)-|c_2|^2\sin 2\theta_i\sin 2\theta(x)\cos\left(\frac{2}{\lambda}\mathrm{Re}I_p(x_i,x_0)+\alpha\right)\\&\times\cos\left(\frac{2}{\lambda}\mathrm{Re}I_p(x,x_0)-\alpha\right)+|c_1|c_2\cos 2\theta_i\sin 2\theta(x)\cos\left(\frac{2}{\lambda}\mathrm{Re}I_p(x,x_0)-\alpha\right).\end{aligned} \tag{3.32}$$

This, along with Eqs. (3.21) and (3.22), is our main result. Recall that in our approximation, c_2 is real. In general, the phase α should be extracted from c_1 directly, rather than taken from the asymptotic series for α given above. This simple form for the survival probability can be evaluated easily and rapidly, providing accurate results for both the direct and interference terms for all mixing parameters except for the extreme nonadiabatic limit. It is much more convenient than direct numerical solution of the MSW equations, especially if many values of the mixing parameters need to be explored.

When $\Omega/\lambda\gg 1$, i.e., the adiabatic limit, $|c_1|\rightarrow 1$, $|c_2|\rightarrow 0$, $\alpha\rightarrow 0$, and this general form for the survival probability reduces to

$$\begin{aligned}P(\nu_e\rightarrow\nu_e)(x,x_i)\rightarrow&\frac{1}{2}[1+\cos 2\theta_i\cos 2\theta(x)]\\&+\frac{1}{2}\sin 2\theta_i\sin 2\theta(x)\cos\left(\frac{2}{\lambda}\mathrm{Re}I_p(x,x_i)\right),\end{aligned} \tag{3.33}$$

which is the usual adiabatic result.

Typically, the final point x will be taken in vacuum, so $\theta(x)\rightarrow\theta_v$ and $\sqrt{\Lambda+\varphi^2(x)}\rightarrow 1$, and

$$\exp\left(\pm\frac{2i}{\lambda}\mathrm{Re}I_p(x,x_0)\right)=\mathrm{const}\times\exp(\pm 2ix/\lambda). \tag{3.34}$$

(The same applies when the lower limit in I_p is x_i, though the constant will be different.) The oscillation length in vacuum is πL, where L is given by Eq. (2.3). For example, in the solar neutrino problem, the favored MSW parameters lead to an oscillation length of $\approx$1000 km [26]. In such cases, where the oscillation length in vacuum is much less than the variation in the source-detector distance, it will be appropriate to average over the detector position. If that is done, then the survival probability no longer depends on x, but does still depend on x_i and is given by

$$\begin{aligned}P(\nu_e\rightarrow\nu_e)(x_i)=&\frac{1}{2}[1+(1-2|c_2|^2)\cos 2\theta_i\cos 2\theta_v]\\&-\frac{1}{2}|c_1|c_2\sin 2\theta_i\cos 2\theta_v\\&\times\cos\left(\frac{2}{\lambda}\mathrm{Re}I_p(x_i,x_0)+\alpha\right).\end{aligned} \tag{3.35}$$

This shows that the source term may be important even after detector averaging. If the source is extended, or if an energy

spectrum is considered, one can also average over the source position. The completely averaged result for the electron survival probability is then given by

$$P(\nu_e \to \nu_e) = \frac{1}{2}[1 + (1-2|c_2|^2)\langle \cos 2\theta_i \rangle_{src} \cos 2\theta(x)], \tag{3.36}$$

where $\langle \cos 2\theta_i \rangle_{src}$ indicates the average of $\cos 2\theta_i$ over the source position and energy spectrum. In the usual derivations, the source term is assumed to be averaged away, yet no average over $\cos 2\theta_i$ is shown. However, one can get away with this in some situations that suppress the source term without any averaging over position or energy.

This structure for the fully averaged survival probability is completely general, and thus we interpret $|c_2|^2$ as the probability of hopping from one mass eigenstate to the other in the passage through the resonance region. Thus,

$$\begin{aligned} P_{\rm hop} &= |c_2|^2 \\ &= \exp(-\pi\Omega) \\ &= \exp\left(-2i \int_{x_0}^{x_0^*} dx \sqrt{\zeta^2(x) - 2\cos 2\theta_v \zeta(x) + 1} \right) \\ &= \exp\left(-i \frac{\delta m^2}{2E} \int_{t_0}^{t_0^*} dt \left\{ \left[\frac{2\sqrt{2} G_F E N_e(t)}{\delta m^2} \right]^2 \right.\right. \\ &\quad \left.\left. - 2\cos 2\theta_v \left[\frac{2\sqrt{2} G_F E N_e(t)}{\delta m^2} \right] + 1 \right\}^{1/2} \right). \end{aligned} \tag{3.37}$$

This probability characterizes the nonadiabatic nature of the evolution near the avoided level crossing; for purely adiabatic evolution, $P_{\rm hop} = 0$. The limits of the integral are the complex turning points of Eq. (A1), i.e., the zeros of the integrand, and are labeled such that $\mathrm{Im} x_0 > 0$. The middle form is particularly convenient since then the turning points are located by $\zeta = \exp(\pm 2i\theta_v)$. This result for $P_{\rm hop}$ is valid for both arbitrary mixing parameters and an arbitrary monotonic density profile. Since our solutions were based on the solution for a linear density, the form of $P_{\rm hop}$ follows that for a linear density: a single exponential which vanishes in the adiabatic limit.

F. Comparisons of different densities

For a linear density, we must recover the linear Landau-Zener result [11,12]. Equation (3.37) yields

$$P_{\rm hop}^{\rm lin} = \exp(-\pi\Omega^{\rm lin}), \tag{3.38}$$

where

$$\Omega^{\rm lin} = \frac{\gamma_c}{2} = \frac{\delta m^2}{4E} \frac{\sin^2 2\theta_v}{\cos 2\theta_v} \left| \frac{1}{N(t)} \frac{dN(t)}{dt} \right|_{\rm res}^{-1}, \tag{3.39}$$

as expected.

For an exponential density, Eq. (3.37) yields

$$P_{\rm hop}^{\rm exp} = \exp(-\pi\Omega^{\rm exp}), \tag{3.40}$$

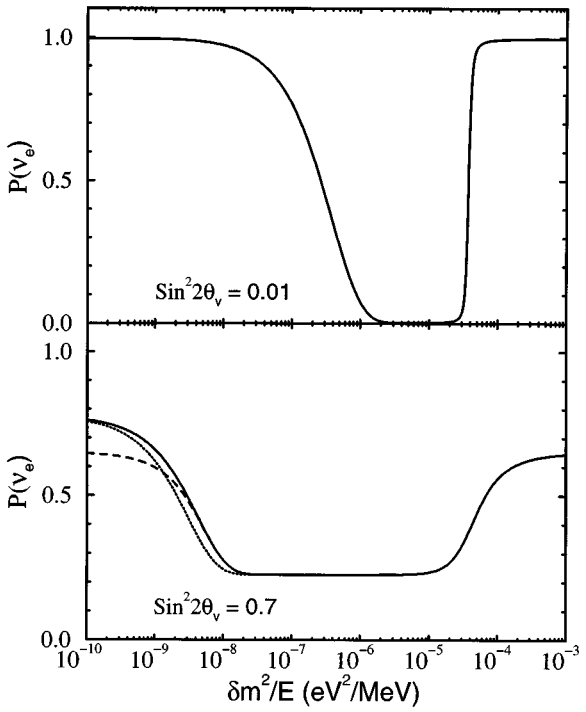

FIG. 1. The electron neutrino survival probability vs the mass-squared difference parameter for two different vacuum-mixing angles. The solid line is given by the method of this paper. The dashed line is the exact (numerical) result. The dotted line is the linear Landau-Zener result. In the top figure, the lines are indistinguishable. An exponential density with parameters chosen to approximate the Sun was used [30]. The region leftward of the lower left corner of the trough is the nonadiabatic region.

where

$$\Omega^{\rm exp} = \delta(1 - \cos 2\theta_v) \tag{3.41}$$

and

$$\delta = \frac{\delta m^2}{2E} \left| \frac{1}{N(t)} \frac{dN(t)}{dt} \right|^{-1}. \tag{3.42}$$

This is the leading exponential to the exact result for an exponential density [13,27]. The exact result is

$$P_{\rm hop}^{\rm exp} = \frac{\exp[-\pi\delta(1-\cos 2\theta_v)] - \exp(-2\pi\delta)}{1 - \exp(-2\pi\delta)}. \tag{3.43}$$

Equation (3.40) for the exponential density was previously obtained [28] by connecting the coefficients of the coupled equations in the adiabatic basis through the complex plane [29]. In Fig. 1, we compare our fully averaged result for the survival probability in an exponential density (the parameters are chosen to approximate the solar density [30]) with the exact result. The values of the vacuum angle chosen approximate those of the two best-fit models for the MSW solution to the solar neutrino problem [26]. In Figs. 2 and 3, we show the accuracy of our approximation by comparing our source term to the exact results. The source term is defined as the survival probability, averaged over detector, minus the survival probability, averaged over both source and detector. Note that in Eq. (3.36), when $\delta m^2/E$ is large, Ω is large, and $c_2 \to 0$, suppressing the source term. On the other hand, if the initial density is large enough, then when $\delta m^2/E$ is small,

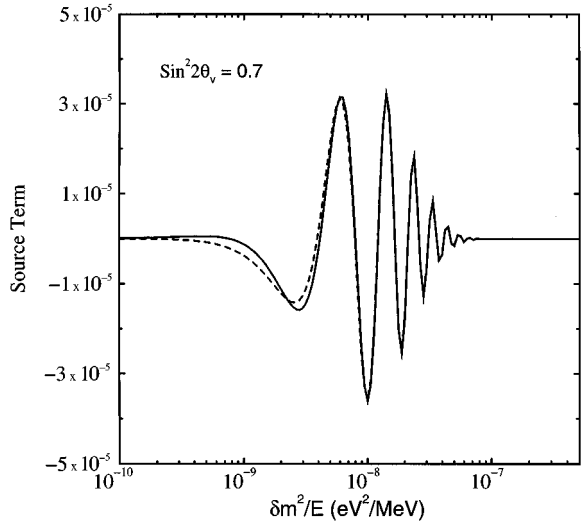

FIG. 2. The source term (the survival probability, averaged over detector, minus the survival probability, averaged over both source and detector) in the electron neutrino survival probability vs the mass-squared difference parameter for $\sin^2 2\theta_v = 0.7$. The solid line is given by the method of this paper. The dashed line is the exact (numerical) result. The density profile is as in Fig. 1.

$\theta_i \to \pi/2$, and $\sin 2\theta_i \to 0$, which also suppresses the source term. Therefore, the source term is nonzero only for intermediate values of δm^2, as illustrated in Figs. 2 and 3.

G. Breakdown of the mapping

As can be seen from Fig. 1, our approximation does not hold in the extreme nonadiabatic limit, where $\delta m^2 \to 0$. As emphasized in Ref. [31], the Miller-Good method only works well when the mapping is invertible. Given two potentials V_A and V_B, the mapping is good only if it makes as much sense to map $V_A \to V_B$ as $V_B \to V_A$. If this is not true, then the mapping is a projection, and something is lost. Invertibility may thus be associated with a ''sameness of topology.'' More precisely, when the mapping is not invertible, the comparison potential becomes multivalued.

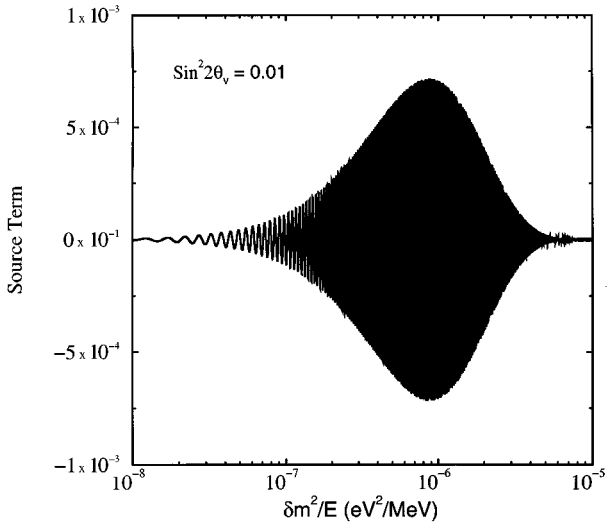

FIG. 3. The source term (the survival probability, averaged over detector, minus the survival probability, averaged over both source and detector) in the electron neutrino survival probability vs the mass-squared difference parameter for $\sin^2 2\theta_v = 0.01$. The solid line is given by the method of this paper. The dashed line is the exact (numerical) result. The lines are indistinguishable, even when a zoom is performed in the region of rapid oscillations. The density profile is as in Fig. 1.

Let us consider the treatment of an exponential density. In this case, the root of the failure in mapping is the difference in the topology of higher-order turning points of the two potentials corresponding to linear and exponential densities. The turning points are located by $\zeta = \exp(\pm 2i\theta_v)$. For a linear density, there are only two turning points. For an exponential density, however, additional, higher-order turning points can be found by the transformation $x \to x + 2\pi n x_s$, where n is an integer and x_s is the scale height of the exponential in our dimensionless units. As noted in Appendix, we considered only the primary turning points, i.e., those closest to the real axis. When only the lowest-order turning points of the exponential density are taken into account, then the two potentials can be made only approximately equivalent. In principle, the way to cure this problem is to use a comparison potential with the same number (infinite, if necessary) of turning points as the original one. In practice, this may be rather cumbersome.

Consider how a path in the x plane is mapped into the S plane. In Appendix, we discuss why the locations of the primary turning points are only considered to lowest order in λ. In particular, the turning points in the S plane are located by $S(x_0) \approx S_0(x_0) = +i\sqrt{\Omega}$, $S^*(x_0) \approx S_0^*(x_0) = -i\sqrt{\Omega}$. The resonance point x_c is mapped to $S(x_c) \approx 0$. In the extreme adiabatic limit, the path from $-\infty$ to $+\infty$ along the real axis in the x plane is mapped onto a path from $-\infty$ to $+\infty$ along the real axis in the S plane. As the mixing parameters become more and more nonadiabatic, the path in the S plane makes more and more of an excursion into one half (upper or lower) of the complex plane near the resonance. At $\pm\infty$, it returns to the real axis. In both planes, the paths run between the primary turning points. In the extreme nonadiabatic limit, however, the path of $S(x)$ eventually crosses a turning point. There is then a topological difference between the two planes; in one case, the path runs between the primary turning points, and in the other, it does not. Because of how the turning points are anchored, this indicates that the mapping has folded the complex plane over, and the comparison potential is multivalued.

The need to impose the same turning point topology between the original and comparison potentials restricts the applicability of Eq. (3.37) to monotonically varying electron densities, i.e., those with a single MSW resonance. If there are two or more close MSW resonances, one cannot use a linear density to construct the comparison potential. Such situations are considered in Refs. [25,32].

IV. CONCLUDING REMARKS

We have studied a uniform semiclassical approximation for the matter-enhanced neutrino oscillations for two flavors, assuming a monotonically changing but otherwise arbitrary density profile. We obtained an analytic expression for the electron neutrino survival probability, unaveraged over either detector or source positions. Our result is valid for a large

range of the mixing parameters, up to but not including the extreme nonadiabatic limit. Upon averaging over detector and source positions, we recover expressions previously obtained in the literature. Since our expressions are valid for arbitrary densities, they may be applied not only to the Sun, but to all settings in which resonant neutrino conversion can occur, such as supernovas and the early Universe.

The method of analytic continuation utilized in Ref. [28] for an exponential density was extended in Ref. [33], where the general form of Eq. (3.37) for an arbitrary monotonic density profile was found. Results for several other analytically solvable densities are presented there. Our analysis not only yields an expression for the hopping probability which coincides with Ref. [33], but also provides the source and detector terms.

As noted, we assumed a monotonic density profile, so this formalism is not suitable for studying neutrino propagation in stochastic media (e.g., with density fluctuations), as has recently been studied for the Sun and type-II supernovas in Refs. [32,34].

ACKNOWLEDGMENTS

We thank J. M. Fetter and R. E. Meyer for helpful discussions. This research was supported in part by the U.S. National Science Foundation Grant No. PHY-9314131 at the University of Wisconsin, and in part by the University of Wisconsin Research Committee with funds granted by the Wisconsin Alumni Research Foundation.

APPENDIX: SUPERSYMMETRY-INSPIRED UNIFORM APPROXIMATION

1. General treatment

Consider the Schrödinger-type equation

$$-\lambda^2 \frac{\partial^2 \Psi(x)}{\partial x^2} - [\Lambda + \varphi^2(x) + i\lambda\,\eta\varphi'(x)]\Psi(x) = 0, \qquad \text{(A1)}$$

where Λ is a real, positive constant, and φ is a real, monotonic function on the real axis, and is analytic in the complex plane. In the above and what follows, everything is dimensionless, and λ is being used as a placeholder for $\hbar$. Neither Λ nor φ depends on λ. We will solve this equation in an approximation that treats λ as formally small. In the physical problem represented by Eq. (A1), the variable x is real. However, for addressing the mathematical question of the solution of this differential equation, we consider x to be complex. We assume[2] that $\Lambda + \varphi^2(x)$ has two zeros in the complex plane, i.e., points x_0, x_0^* where $\varphi = \pm i\sqrt{\Lambda}$. These points are taken to be the turning points of Eq. (A1). We will discuss below why the turning points can be taken at lowest order, i.e., given as the zeros of $\Lambda + \varphi^2(x)$, rather than of $\Lambda + \varphi^2(x) + i\lambda\,\eta\varphi(x)$. In general, there can be more than two zeros of $\Lambda + \varphi^2$; for now, we only consider the two closest to the real axis, and label them so that $\mathrm{Im}x_0 > 0$. The overall sign on φ is chosen to make $\mathrm{Im}\varphi(x_0) > 0$, and η is taken to be ± 1 as needed so that $\eta\varphi(x)$ has the desired sign. If presented with an equation such as Eq. (A1), but with the opposite sign on the imaginary term, one can always conjugate it and solve as below for $\Psi^*(x)$, so the treatment here is general.

We will map Eq. (A1) onto the comparison equation

$$-\lambda^2 \frac{\partial^2 U(S)}{\partial S^2} - [\Omega + S^2 + i\lambda\,\eta]U(S) = 0\,, \qquad \text{(A2)}$$

where Ω is a real, positive constant (and will be determined below). This equation, considered as a function of S, also has two conjugate turning points in the complex plane. By ''map,'' we mean that we will find a change of variables $S = S(x)$ such that the potential in the comparison equation is deformed into the potential in the original equation. That statement indicates how the real axis will be stretched. However, we will also have to consider how the complex x plane is mapped onto the complex S plane. In particular, the turning points in the x plane must be mapped onto the turning points in the S plane. The comparison equation is chosen to be one for which exact analytic solutions are known, and which is as similar as possible to the original equation. If we require $\varphi(x)$ to be monotonic for real x, then imaginary term in the comparison equation may be taken as constant. Other than Ω, this comparison equation is taken with no free parameters; such parameters can always be scaled away, and so are irrelevant here. That the turning-point topologies of the original and comparison problems be the same is critical to the method. In this case, we are mapping an as-yet unspecified real barrier onto a parabolic barrier, and the imaginary term onto an imaginary constant. However, we can map onto any convenient potential with known solutions.

In principle, if we could find the change of variables $S = S(x)$ exactly, then we would have exact solutions for $\Psi(x)$ in terms of the known functions $U(S(x))$. In general, the solution for the change of variables $S = S(x)$ would be at least as difficult as direct solution of the original problem. The approximation made to solve Eq. (A1) will be to approximate $S(x)$ as a truncated power series in λ. This method of uniform approximation via mapping is also known as the method of comparison equations (note Ref. [35]). The work here was inspired by the ideas of Miller and Good [16]. For further work on the theory of their method, see also Refs. [36,31], and the related works in Ref. [37].

In the original Miller-Good problem, the imaginary terms in the potentials above are not present. They treat the cases of a particle bound in a well and traveling in the presence of a barrier, mapping onto a parabolic well and barrier, respectively, each of which has as solutions the parabolic cylinder functions. In their formalism, one immediately sees that the WKB approximation amounts to mapping onto the free-particle potential; the mismatch in turning-point topologies is the origin of the failure of the WKB method [via the zeros in what is essentially a Jacobian, see Eq. (A19)] near the turning points. With the Miller-Good formalism, the wave function is continuous through the turning points.

The notation used here has some important differences from previous work [6,8]. This allows some difficulties and errors to be resolved. In particular, η will be used differently

[2]The case in which the zeros are on the real axis, while not relevant here, can be treated similarly to the rest of the Appendix; see Ref. [6].

here. We continue to take $\varphi(x)$ to be real on the real axis and to be monotonic. In those papers, it was assumed that $\varphi(x)$ monotonically increasing along the real axis would imply $\mathrm{Im}\varphi(x_0)>0$. While this is suggested by the Cauchy-Riemann conditions applied to $\varphi(x)$ on the real axis, it need not always be true. No such assumption is made here. For each density, one simply has to make sure that the signs of $\varphi(x)$ and η are defined so that $\eta\varphi(x)$ represents the right physics and that $\mathrm{Im}\varphi(x_0)>0$.

This mapping will be accomplished as

$$\Psi(x)=K(x)U(S(x)), \tag{A3}$$

where the form of $K(x)$ will be chosen and $S(x)$ will be defined by that choice. Using this form of $\Psi(x)$ and Eq. (A2), we can rewrite Eq. (A1). By making the choice

$$K(x)=\frac{1}{\sqrt{S'(x)}}, \tag{A4}$$

and dividing through by Ψ, we find

$$\lambda^2\frac{K''}{K}-S'^2[\Omega+S^2+i\lambda\,\eta]+[\Lambda+\varphi^2+i\lambda\,\eta\varphi']=0\,. \tag{A5}$$

So far, no approximation has been made, and the form

$$\Psi(x)=\frac{1}{\sqrt{S'(x)}}U(S(x)) \tag{A6}$$

is a purely formal solution of Eq. (A1) in terms of the solutions of Eq. (A2). If we could find the change of variables $S=S(x)$ exactly, then we would have exact solutions for $\Psi(x)$ in terms of the known functions $U(S(x))$. In general, the solution for the change of variables $S=S(x)$ would be at least as difficult as direct solution of the original problem. To avoid that, we will approximate $S(x)$. Very crudely, this procedure is a perturbation expansion in the shapes of the two potentials; the more they resemble each other, the more our approximation to the change of variables is justified, and the better our solutions $\Psi(x)$ will be. Since φ is independent of λ, all of the λ dependence in Eq. (A5) is explicit. We expand $S(x)$ in powers of λ:

$$S(x)=S_0(x)+\lambda S_1(x)+\cdots. \tag{A7}$$

The power of this method is that we can obtain a good solution by keeping only the semiclassical terms (the lowest two orders in λ). In the original Miller and Good problem [16], the $i\lambda\varphi'$ term was not present in the potential. Therefore, only λ^2 appears in Eq. (A5), and one can expand in λ^2 instead of λ, which leads to $S(x)\approx S_0(x)+O(\lambda^2)$, making solving for the mapping quite simple. In our case, since λ appears directly in Eq. (A5), we must expand in λ, which leads to

$$S(x)\approx S_0(x)+\lambda S_1(x), \tag{A8}$$

which makes solution of the mapping somewhat more complicated, but still much easier to solve than the original equation. After expansion of Eq. (A5) in λ, we group by order in λ and demand that each order vanishes independently, as λ is a free parameter as far as the mathematics are concerned. This yields the equations

$$\begin{aligned} &O(\lambda^0): \quad (\Lambda+\varphi^2)=S_0'^2(\Omega+S_0^2),\\ &O(\lambda^1): \quad i\eta\varphi'=2(\Omega+S_0^2)S_0'S_1'+S_0'^2(i\eta+2S_0S_1). \end{aligned} \tag{A9}$$

While the original equation to be solved was linear, after approximation the system of equations to be solved is nonlinear. In particular, the equation for the $O(\lambda^2)$ terms, which involves $S_2(x)$, is probably analytically intractable. Nevertheless, the integrations for $S_0(x)$ and $S_1(x)$ can be performed, and the results are given below. In those integrations, the branch cut for the logarithm and square-root functions is taken along the negative real axis. Before solving for $S_0(x)$ and $S_1(x)$, we show what will be left over. Using the relations for $S_0(x)$ and $S_1(x)$, one can show

$$-\lambda^2\frac{\partial^2\Psi_{\mathrm{appr}}(x)}{\partial x^2}-[\Lambda+\varphi^2(x)+i\lambda\,\eta\varphi'(x)+\lambda^2\epsilon(x)]\times\Psi_{\mathrm{appr}}(x)=0. \tag{A10}$$

In the rest of the Appendix, $\Psi(x)$ always denotes the approximate wave function, and we drop the subscript. The degree to which the approximate solution fails to solve the exact differential equation is the local error, and is of the form

$$\epsilon(x)=\frac{3}{4}\left(\frac{S_0''}{S_0'}\right)^2-\frac{1}{2}\left(\frac{S_0'''}{S_0'}\right)-S_0'^2S_1^2-2S_0'S_1'(i\eta+2S_0S_1)-S_1'^2(\Omega+S_0^2)+(\text{terms that depend on } S_2). \tag{A11}$$

The first two terms are familiar from either the WKB [38] or Miller-Good [16] problems.[3] The next three terms arise from the more general form of the potential considered here. Unfortunately, the remaining terms depend on S_2, for which we have no analytic solution.

The turning points of the original and comparison equations are taken to be the zeros of $[\Lambda+\varphi^2(x)]$ and $[\Omega+S^2(x)]$, respectively. Since these are real for real x, the turning points are complex conjugates. As noted above, the turning points of original equation are labeled so that $\mathrm{Im}x_0>0$, and the sign of $\varphi(x)$ is chosen so that $\varphi(x_0)=i\sqrt{\Lambda}$. We map the turning points of the original equation onto the turning points of the comparison equation by demanding $S(x_0)=i\sqrt{\Omega}$. The way this correspondence is made ensures that the mapping does not flip the complex plane about the real axis (it is not flipped about the imaginary axis either, as will be shown below). These choices make it easier to avoid integration errors below. Note that all of the turning points are treated only at lowest order.

[3]While these methods have the same form for the local error, the global results can be rather different, e.g., the transmission coefficient [16]. Note that the WKB error term is singular at the turning points, whereas the Miller-Good error term is bounded.

The formal solution for $S_0(x)$ can be written immediately from Eq. (A9), including the turning-point correspondence condition of $S_0(x_0)=i\sqrt{\Omega}$:

$$I_p(x,x_0)\equiv\int_{x_0}^{x}dx\sqrt{\Lambda+\varphi^2(x)}=\int_{i\sqrt{\Omega}}^{S_0(x)}dS_0\sqrt{\Omega+S_0^2}. \quad \text{(A12)}$$

In order to evaluate $S_0(x)$, we will first need Ω, the energy of the comparison system. This is determined by demanding that the conjugate turning points correspond, i.e., $S_0(x_0^*)=-i\sqrt{\Omega}$. When both sides of Eq. (A12) are integrated between their turning points, the right-hand side can be done explicitly, yielding

$$-\frac{i\Omega\pi}{2}=\int_{x_0}^{x_0^*}dx\sqrt{\Lambda+\varphi^2(x)}. \quad \text{(A13)}$$

With Ω determined, an implicit solution for $S_0(x)$ can be obtained through integration of Eq. (A12) to a general point x:

$$I_p(x,x_0)=-\frac{i\Omega\pi}{4}+\frac{S_0}{2}\sqrt{\Omega+S_0^2}+\frac{\Omega}{2}\ln\left(\frac{S_0+\sqrt{\Omega+S_0^2}}{\sqrt{\Omega}}\right). \quad \text{(A14)}$$

The fact that the solution for $S_0(x)$ is left in this implicit form does not present any difficulties. When the asymptotic forms are used, this expression can be solved approximately. If the full forms of the parabolic cylinder functions are being used, then one will be taking a numerical approach anyway, and the solution for $S_0(x)$ is rather easy. Using the Schwarz reflection principle and the integrals for $S_0(x)$ and Ω, one can show that $S_0(x)$ is real for real x. Then, $I_p(x,x_0)$ separates into real and imaginary parts as follows:

$$I_p(x,x_0)=\mathrm{Re}[I_p(x,x_0)]-\frac{i\Omega\pi}{4}. \quad \text{(A15)}$$

This will be needed to show that the exponentials in the asymptotic solution have purely imaginary arguments.

To solve for $S_1(x)$, we use the first of Eq. (A9) to rewrite the second as

$$\frac{i\eta}{2}\frac{\varphi'}{\sqrt{\Lambda+\varphi^2}}=S_1'\sqrt{\Omega+S_0^2}+\frac{1}{2}\frac{S_0'}{\sqrt{\Omega+S_0^2}}(i\eta+2S_0S_1). \quad \text{(A16)}$$

We integrate from x_0 to x, changing variables as needed

$$\frac{i\eta}{2}\int_{\varphi(x_0)}^{\varphi(x)}\frac{d\varphi}{\sqrt{\Lambda+\varphi^2}}=\int_{x_0}^{x}dx\frac{d}{dx}(S_1\sqrt{\Omega+S_0^2})+\frac{i\eta}{2}\int_{S_0(x_0)}^{S_0(x)}\frac{dS_0}{\sqrt{\Omega+S_0^2}}. \quad \text{(A17)}$$

In all three integrals, the lower limit has a positive imaginary part and the upper limit is real; this ensures that all of the square-root functions are on the same sheet. Upon substitution of the limits of integration, this yields

$$S_1(x)=\frac{i\eta}{2\sqrt{\Omega+S_0^2}}\left\{\ln\left[\frac{\varphi+\sqrt{\Lambda+\varphi^2}}{\sqrt{\Lambda}}\right]+\ln\left[\frac{\sqrt{\Omega}}{S_0+\sqrt{\Omega+S_0^2}}\right]\right\}, \quad \text{(A18)}$$

which is purely imaginary for real x, as claimed in Refs. [7,8]. In those references, there were typographical errors (corrected here), and this was not obvious. In order to get S_1 right (i.e., pure imaginary), one has to be careful about a branch cut crossing during the integration. In order to facilitate that, φ is defined here with the sign noted in Eq. (2.5).

The prefactor $K(x)$ is given by

$$K(x)=\frac{1}{\sqrt{S'(x)}}\approx\frac{1}{\sqrt{S_0'(x)}}=\left[\frac{\Omega+S_0^2(x)}{\Lambda+\varphi^2(x)}\right]^{1/4}. \quad \text{(A19)}$$

The truncation of S' at lowest order here is consistent with our overall policy of keeping the two lowest orders in λ, and will be justified below. This form allows us to explain why the turning points may be taken at lowest order. Consider how the exact change of variables $S=S(x)$ would work at a single point, where the local momenta in both problems could be taken as constant. Then the change of variables is just a scale change, and $K^2(x)$ is the ratio of the exact local momenta, the zeros of which are the exact turning points. When we approximate $S(x)$ by power series in λ, $K^2(x)$ will be the ratio of the local momenta, taken at the proper order, the zeros of which are the turning points, taken at the proper order. From the expression for $K(x)$ above, this indicates that the turning points should be taken at the lowest order in λ. The denominator of $K(x)$ vanishes at the turning points. For there to be any hope of $\Psi(x)$ being well behaved at the turning points, the numerator must also vanish. This is why we demanded the turning-point matching as above. In the WKB case, the numerator never vanishes, and the connection between the mismatch in turning-point topologies and the singularity of the WKB solutions at the turning points is evident. When the turning points are matched properly, one can show that $K(x)$ is well behaved for all x. The method of proof is to expand Eq. (A12) near one turning point; this reveals that $K(x)$ tends to a constant as the turning point is approached. The same holds for the other turning point as well.

After successively solving for Ω, $S_0(x)$, $S_1(x)$, and $K(x)$, one can write the approximate wave function as

$$\Psi(x)=\left[\frac{\Omega+S_0^2(x)}{\Lambda+\varphi^2(x)}\right]^{1/4}U(S_0(x)+\lambda S_1(x)), \quad \text{(A20)}$$

where $U(S_0(x)+\lambda S_1(x))$ approximately solves Eq. (A2), the comparison equation, and $\Psi(x)$ approximately solves Eq. (A1), the original Schrödinger-type equation. By taking

$$z(x)=\frac{1+i}{\sqrt{\lambda}}S(x)\approx\frac{1+i}{\sqrt{\lambda}}(S_0(x)+\lambda S_1(x)), \quad \text{(A21)}$$

one can show that Eq. (A2) is Weber's equation [19–21] for the parabolic cylinder function $D_\nu(z)$, where the order ν is given by

$$\nu=\frac{\eta-1-i\Omega/\lambda}{2}. \tag{A22}$$

The general solution may be taken to be

$$\Psi(x)=K(x)[AD_\nu(z(x))+BD_\nu(-z(x))]. \tag{A23}$$

There are four solutions to Weber's equation, any two of which can be taken as independent; the two above are convenient. Given appropriate initial conditions, one can solve for $\Psi(x)$ everywhere. The coefficients A and B will be determined below by applying the initial conditions to the asymptotic form of the solution. The evaluation of the parabolic cylinder functions is discussed in the body of the paper.

2. Asymptotic forms

In many cases, one only needs the wave function as $x\rightarrow\pm\infty$ (the reasons for this in the MSW problem are explained in the body of the paper). In this section, we develop the asymptotic forms of $\Psi(x)$, which are easier to work with than the general form above. Another benefit of the asymptotic forms is that it becomes much easier to count powers of λ, thus ensuring that we are working to a consistent order.

Using the definitions in the previous section, one can easily show

$$S_0(x)\underset{x\rightarrow\pm\infty}{\sim}\pm\infty \tag{A24}$$

and

$$S_1(x)\underset{x\rightarrow\pm\infty}{\sim}0. \tag{A25}$$

With these crude limits, and the fact that $S_0(x)$ is real for real x, we can determine the phases to the arguments of $D_\nu(z(x))$ and $D_\nu(-z(x))$ to be $\pi/4$ and $-3\pi/4$, respectively, for $x\rightarrow+\infty$, and vice versa for $x\rightarrow-\infty$. We use $-3\pi/4$ instead of $5\pi/4$ to stay inside the principal branches of the square-root and logarithm functions used below. In particular, one must be careful when rewriting z^ν. The asymptotic forms of the parabolic cylinder functions for $|z|\gg|\nu|$ are given in Ref. [20]. For $-3\pi/4<\arg(z)<3\pi/4$,

$$D_\nu(z)\underset{z\rightarrow\infty}{\sim}\exp\left(-\frac{z^2}{4}\right)z^\nu\left[1+O\left(\frac{1}{z^2}\right)\right] \tag{A26}$$

and for $-5\pi/4<\arg(z)<-\pi/4$,

$$D_\nu(z)\underset{z\rightarrow\infty}{\sim}\exp\left(-\frac{z^2}{4}\right)z^\nu\left[1+O\left(\frac{1}{z^2}\right)\right]-\frac{\sqrt{2\pi}}{\Gamma(-\nu)}e^{-i\nu\pi}\exp\left(\frac{z^2}{4}\right)z^{-\nu-1}\left[1+O\left(\frac{1}{z^2}\right)\right]. \tag{A27}$$

In the common range of validity, the difference between the two forms is negligibly small.

These asymptotic forms make the dependence upon λ in the various terms easy to see, and show how to keep consistent orders in λ. As befits our semiclassical expansion, we only keep the lowest two orders in λ in the exponentials of the asymptotic wave functions. Using the form of z given in Eq. (A21),

$$\exp\left(\pm\frac{z^2}{4}\right)=\exp\left[\pm\frac{i}{2}\left(\frac{S_0^2}{\lambda}+2S_0S_1+O(\lambda)\right)\right], \tag{A28}$$

$$z^\nu=\left(\frac{1+i}{\sqrt{\lambda}}\right)^\nu S_0^\nu\exp\left(-\frac{i\Omega}{2}\frac{S_1}{S_0}+O(\lambda)\right), \tag{A29}$$

$$z^{-\nu-1}=\left(\frac{1+i}{\sqrt{\lambda}}\right)^{-\nu-1}S_0^{-\nu-1}\exp\left(+\frac{i\Omega}{2}\frac{S_1}{S_0}+O(\lambda)\right), \tag{A30}$$

$$1+O\left(\frac{1}{z^2}\right)=\exp(O(\lambda)), \tag{A31}$$

$$K(x)=\frac{1}{\sqrt{S'(x)}}=\frac{1}{\sqrt{S_0'(x)}}\exp(O(\lambda)). \tag{A32}$$

Now, we expand the various pieces for large $|x|$. Using Eq. (A14), and keeping only terms growing or constant in $|S_0(x)|$, one can easily show

$$\frac{S_0^2(x)}{2\lambda}\underset{x\rightarrow\pm\infty}{\sim}\pm\frac{I_p(x,x_0)}{\lambda}+\frac{(\pm i\pi-1)\Omega}{4\lambda}+\frac{\Omega}{4\lambda}\ln\left(\frac{\Omega}{\lambda}\right)-\frac{\Omega}{2\lambda}\ln\left(\frac{2|S_0(x)|}{\sqrt{\lambda}}\right). \tag{A33}$$

When $|S_0|\gg\Omega$ and this expansion is valid, then $|z|\gg|\nu|$ and the D_ν's can be put in their asymptotic forms. Using Eq. (A15), one can see that S_0^2 is purely real for real x, as claimed. The various λ terms were introduced to show where $\hbar$'s would appear if we took these equations out of dimensionless form. The expansion for S_1 from Eq. (A18) is straightforward, and yields

$$S_1(x)\underset{x\rightarrow\pm\infty}{\sim}\frac{i\eta}{2|S_0|}\left\{\ln\left[\frac{\varphi+\sqrt{\Lambda+\varphi^2}}{\sqrt{\Lambda}}\right]\mp\ln\left(\frac{\sqrt{\lambda}}{\sqrt{\Omega}}\right)\mp\ln\left(\frac{2|S_0|}{\sqrt{\lambda}}\right)\right\}. \tag{A34}$$

In this expansion, $|S_0|$ was treated asymptotically but $|\varphi|$ was not. [At the MSW resonance point discussed in the body of this paper, $\varphi(x_c)=0$ but $S_0(x_c)\neq0$ in general.] The nonadiabatic region is, in general, far narrower than the region over which the matter angle is varying appreciably. The region in which S_0 cannot be treated asymptotically is essentially the nonadiabatic region, whereas φ cannot be treated asymptotically until the matter angle is very close to either $\pi/2$ or θ_v. We expand $K(x)$ as

$$K(x) \underset{x\to\pm\infty}{\sim} \left(\frac{\lambda}{\Lambda}\right)^{1/4}\left[\frac{\Lambda}{4[\Lambda+\varphi^2(x)]}\right]^{1/4} \times \exp\left[\frac{1}{2}\ln\left(\frac{2|S_0(x)|}{\sqrt{\lambda}}\right)\right]. \quad \text{(A35)}$$

The factors of $|S_0(x)|$ remaining in these asymptotic expansions will all cancel.

For convenience in applying the initial conditions, it is useful to write

$$I_p(x,x_0) = I_p(x_i,x_0) + I_p(x,x_i), \quad \text{(A36)}$$

where the first term on the right is a complex constant and the second is real and varying [cf. Eq. (A15)]. After some algebra, we find that the asymptotic expansion of the general solution in Eq. (A23) can be written as

$$\Psi(x) \underset{x\to\pm\infty}{\sim} \left[\frac{\Lambda}{4[\Lambda+\varphi^2(x)]}\right]^{1/4} \times \left\{ C_\pm \left(\frac{\varphi+\sqrt{\Lambda+\varphi^2}}{\sqrt{\Lambda}}\right)^{\pm\eta/2} \exp\left(\mp\frac{i}{\lambda} I_p(x,x_i)\right) + D_\pm \left(\frac{\varphi+\sqrt{\Lambda+\varphi^2}}{\sqrt{\Lambda}}\right)^{\mp\eta/2} \exp\left(\pm\frac{i}{\lambda} I_p(x,x_i)\right)\right\}. \quad \text{(A37)}$$

In the arguments of the exponentials, all terms of $O(\lambda)$ or that vanish as $|x|\to\infty$ have been dropped. The constant coefficients are given by

$$C_+ = C\exp\left(-\frac{i}{\lambda}\mathrm{Re}I_p(x_i,x_0)\right)(A+Be^{-i\nu\pi}), \quad \text{(A38)}$$

$$C_- = C\exp\left(+\frac{i}{\lambda}\mathrm{Re}I_p(x_i,x_0)\right)(Ae^{-i\nu\pi}+B), \quad \text{(A39)}$$

$$D_+ = D\exp\left(+\frac{i}{\lambda}\mathrm{Re}I_p(x_i,x_0)\right)(Be^{-i\nu\pi}), \quad \text{(A40)}$$

$$D_- = D\exp\left(-\frac{i}{\lambda}\mathrm{Re}I_p(x_i,x_0)\right)(Ae^{-i\nu\pi}), \quad \text{(A41)}$$

and

$$C = \left(\frac{\lambda}{\Lambda}\right)^{1/4}\left(\frac{\Omega}{\lambda}\right)^{-i\Omega/4\lambda+\eta/4}\left(\frac{e^{i\pi/4}}{\sqrt{2}}\right)^{\nu}\exp\left(\frac{i\Omega}{4\lambda}\right), \quad \text{(A42)}$$

$$D = -\frac{\sqrt{2\pi}}{\Gamma(-\nu)}\left(\frac{\lambda}{\Lambda}\right)^{1/4}\left(\frac{\Omega}{\lambda}\right)^{+i\Omega/4\lambda-\eta/4}\left(\frac{e^{-3i\pi/4}}{\sqrt{2}}\right)^{-\nu-1} \times \exp\left(-\frac{i\Omega}{4\lambda}\right). \quad \text{(A43)}$$

Note that the arguments to the x-dependent exponentials above are purely imaginary since $I_p(x,x_i)$ is real (that knowledge will be convenient when we take the squared modulus of the wave function).

[1] S.P. Mikheyev and A.Yu. Smirnov, Sov. J. Nucl. Phys. **42**, 913 (1985); Sov. Phys. JETP **64**, 4 (1986); L. Wolfenstein, Phys. Rev. D **17**, 2369 (1978); **20**, 2634 (1979).

[2] J.N. Bahcall, *Neutrino Astrophysics* (Cambridge University Press, New York, 1989); J.N. Bahcall and H.A. Bethe, Phys. Rev. Lett. **65**, 2233 (1990); *Solar Modeling*, edited by A.B. Balantekin and J.N. Bahcall (World Scientific, Singapore, 1995).

[3] W.C. Haxton, Annu. Rev. Astron. Astrophys. **33**, 459 (1995).

[4] G.M. Fuller, R.W. Mayle, B.S. Mayer, and J.R. Wilson, Astrophys. J. **389**, 517 (1992); S.E. Woosley and R. Hoffman, *ibid.* **395**, 202 (1992); S.E. Woosley, G.J. Mathews, J.R. Wilson, R.D. Hoffman, and B.S. Meyer, *ibid.* **433**, 229 (1994); G.M. Fuller, Phys. Rep. **227**, 149 (1993); Y.-Z. Qian, G.M. Fuller, G.J. Matthews, R.W. Mayle, J.R. Wilson, and S.E. Woosley, Phys. Rev. Lett. **71**, 1965 (1993).

[5] O.V. Bychuk and V.P. Spiridonov, Mod. Phys. Lett. A **5**, 1007 (1990).

[6] S.H. Fricke, A.B. Balantekin, P.J. Hatchell, and T. Uzer, Phys. Rev. A **37**, 2797 (1988).

[7] A.B. Balantekin, S.H. Fricke, and P.J. Hatchell, Phys. Rev. D **38**, 935 (1988).

[8] A.B. Balantekin and J.E. Seger, Int. J. Mod. Phys. A **6**, 695 (1991).

[9] V. Barger, R.J.N. Phillips, and K. Whisnant, Phys. Rev. D **34**, 980 (1986).

[10] L. Landau, Phys. Z. Sowjetunion **2**, 46 (1932); C. Zener, Proc. R. Soc. London **A137**, 696 (1932); E.C.G. Stueckelberg, Helv. Phys. Acta **5**, 369 (1932).

[11] W.C. Haxton, Phys. Rev. Lett. **57**, 1271 (1986).

[12] S.J. Parke, Phys. Rev. Lett. **57**, 1275 (1986).

[13] M. Bruggen, W.C. Haxton, and Y.-Z. Qian, Phys. Rev. D **51**, 4028 (1995).

[14] J.C. D'Olivo, Phys. Rev. D **45**, 924 (1992).

[15] J. Heading, *An Introduction to Phase-Integral Methods* (Methuen, London, 1962); J. Mathews and R.L. Walker, *Mathematical Methods of Physics* (Benjamin, Menlo Park, 1970); M.V. Berry and K.E. Mount, Rep. Prog. Phys. **35**, 315 (1972); M.S. Child, *Semiclassical Mechanics with Molecular Applications* (Clarendon, Oxford, 1991).

[16] S.C. Miller, Jr. and R.H. Good, Jr., Phys. Rev. **91**, 174 (1953).

[17] D.W. Lozier and F.W.J. Olver, in *Mathematics of Computation, 1943–1993: a Half-Century of Computational Mathematics*, edited by W. Gautschi (American Mathematical Society, Providence, RI, 1994); an updated version is available at http://math.nist.gov/nesf/.

[18] K.S. Kölbig, Comput. Phys. Commun. **4**, 221 (1972); the li-

brary is available from http://asdwww.cern.ch/pl/index.html.
[19] *Handbook of Mathematical Functions*, edited by M. Abramowitz and I.A. Stegun (Dover, New York, 1972).
[20] E.T. Whittaker and G.N. Watson, *A Course of Modern Analysis* (Cambridge University Press, New York, 1973).
[21] J.C.P. Miller, *Tables of Weber Parabolic Cylinder Functions* (Her Majesty's Stationery Office, London, 1955); *Higher Transcendental Functions* (Bateman Manuscript Project), edited by A. Erdelyi *et al.* (McGraw-Hill, New York, 1953), Vol. II; W. Magnus, F. Oberhettinger, and R.P. Soni, *Formulas and Theorems for the Special Functions of Mathematical Physics* (Springer, Berlin, 1966); note that in the last two references there are errors in the asymptotic forms of the parabolic cylinder functions.
[22] I.Ye. Kireyeva and K.A. Karpov, *Tables of Weber Functions* (Pergamon, New York, 1961).
[23] G. Maino, E. Menapace, and A. Ventura, J. Comput. Phys. **40**, 294 (1981); Z. Schulten, R.G. Gordon, and D.G.M. Anderson, *ibid.* **42**, 213 (1981); G.D. James, Comput. Phys. Commun. **40**, 375 (1986); G. Taubmann, *ibid.* **69**, 415 (1992).
[24] A.C. Hindmarsh and L.R. Petzold, Comput. Phys. **9**, 34 (1995); **9**, 148 (1995).
[25] W.C. Haxton and W.-M. Zhang, Phys. Rev. D **43**, 2482 (1991).
[26] S.A. Bludman, N. Hata, D.C. Kennedy, and P.G. Langacker, Phys. Rev. D **47**, 2220 (1993).
[27] S. Toshev, Phys. Lett. B **196**, 170 (1987); S.T. Petcov, *ibid.* **200**, 373 (1988); S. T. Petcov and J. Rich, *ibid.* **224**, 426 (1989).
[28] P. Pizzochero, Phys. Rev. D **36**, 2293 (1987).
[29] L.D. Landau and E.M. Lifshitz, *Quantum Mechanics: Non-Relativistic Theory*, 2nd ed. (Pergamon, New York, 1975), Sec. 52.
[30] J.N. Bahcall, *Neutrino Astrophysics* (Cambridge University Press, New York, 1989), p. 101.
[31] P. Pechukas, J. Chem. Phys. **54**, 3864 (1971).
[32] A.B. Balantekin, J.M. Fetter, and F.N. Loreti, Phys. Rev. D **54**, 3941 (1996).
[33] T.K. Kuo and J. Pantaleone, Phys. Rev. D **39**, 1930 (1989).
[34] F.N. Loreti and A.B. Balantekin, Phys. Rev. D **50**, 4762 (1994); F.N. Loreti, Y.-Z. Qian, G.M. Fuller, and A.B. Balantekin, *ibid.* **52**, 6664 (1995).
[35] R.E. Langer, Trans. Am. Math. Soc. **67**, 461 (1949).
[36] S.C. Miller, Jr., Phys. Rev. **94**, 1345 (1954); H. Moriguchi, J. Phys. Soc. Jpn. **14**, 1771 (1959); E. Zauderer, J. Chem. Phys. **56**, 5198 (1972); J. Giraldo, R.G. Barrera, and G.A. Estévez, Chem. Phys. Lett. **113**, 37 (1985); J.B. Keller, Am. J. Phys. **54**, 546 (1986); H. Moriguchi, Rep. Fac. Sci. Shizuoka Univ. **24**, 9 (1990).
[37] R.B. Dingle, Appl. Sci. Res. Ser. B **5**, 345 (1956); N.D. Kazarinoff, Arch. Ration Mech. Anal. **2**, 129 (1958); A. Erdélyi, J. Math. Phys. (N.Y.) **1**, 16 (1960); R.Y.S. Lynn and J.B. Keller, Commun. Pure Appl. Math. **23**, 379 (1970); E. Zauderer, Proc. Am. Math. Soc. **31**, 489 (1972); V. Aquilanti, S. Cavalli, and M.B. Sevryuk, J. Phys. A **24**, 4475 (1991).
[38] J. Mathews and R.L. Walker, *Mathematical Methods of Physics* (Benjamin, Menlo Park, 1970), rewrite Eq. (1-95) using Eqs. (1-88).